International Journal of Nanomedicine

Dovepress
open access to scientific and medical research

Open Access Full Text Article

ORIGINAL RESEARCH

Development of surface-engineered PLGA nanoparticulate-delivery system of Tet1-conjugated nattokinase enzyme for inhibition of $A\beta_{40}$ plaques in Alzheimer's disease

This article was published in the following Dove Press journal:
International Journal of Nanomedicine

Prakash Chandra Bhatt,[1] Amita Verma,[2] Fahad A Al-Abbasi,[3] Firoz Anwar,[3] Vikas Kumar,[4] Bibhu Prasad Panda[1]

[1]Microbial and Pharmaceutical Biotechnology Laboratory, Centre for Advanced Research in Pharmaceutical Science, Faculty of Pharmacy, Jamia Hamdard, New Delhi, India; [2]Bioorganic & Medicinal Chemistry Research Laboratory, Department of Pharmaceutical Sciences, Faculty of Health Sciences, Sam Higginbottom University of Agriculture, Technology and Sciences, Allahabad, Uttar Pradesh, India; [3]Department of Biochemistry, Faculty of Science, King Abdulaziz University, Jeddah, Saudi Arabia; [4]Natural Product Drug Discovery Laboratory, Department of Pharmaceutical Sciences, Faculty of Health Sciences, Sam Higginbottom University of Agriculture, Technology and Sciences, Allahabad, Uttar Pradesh, India

Correspondence: Vikas Kumar
Natural Product Drug Discovery Laboratory, Department of Pharmaceutical Sciences, Faculty of Health Sciences, Sam Higginbottom University of Agriculture, Technology and Sciences, Rewa Road, Naini, Allahabad, Uttar Pradesh 211007, India
Email phvikas@gmail.com

Bibhu Prasad Panda
Microbial and Pharmaceutical Biotechnology Laboratory, Centre for Advanced Research in Pharmaceutical Science, Faculty of Pharmacy, Jamia Hamdard, Mehrauli–Badarpur Road, Hamdard Nagar, New Delhi, Delhi 110062, India
Email bibhu_panda31@rediffmail.com

Abstract: According to the World Health Organization, globally there are around 18 million patients suffering from Alzheimer's disease (AD), and this number is expected to double by 2025. The pathophysiology of AD includes selective deposition of Aβ peptide in the mitochondria of cells, which inhibits uptake of glucose by neurons and key enzyme functions. Current drug treatments for AD are unable to rectify the underlying pathology of the disease; they only provide short-term symptomatic relief, so there is a need for the development of newer treatment regimes. The antiamyloid activity, antifibrinolytic activity, and antithrombotic activity of nattokinase holds potential for the treatment of AD. As nattokinase is a protein, its stability restricts its usage to a greater extent, but this limitation can be overcome by nanoencapsulation. In this work, we successfully synthesized polymeric nanoparticles of nattokinase and characterized its use by different techniques: transmission electron microscopy, scanning electron microscopy, DTS Nano, differential scanning calorimetry, Fourier-transform infrared spectroscopy, thioflavin T-binding assay, in vitro drug release, antifibrinolytic activity, and in vivo antiamyloid activity. As brain targeting of hydrophilic drugs is complicated due to the stringent nature of blood–brain barrier, in the current experimental study, we conjugated poly(lactic-*co*-glycolic acid) (PLGA)-encapsulated nattokinase with Tet1 peptide, which exhibits retrograde transportation properties because of its affinity to neurons. Our study suggests that PLGA-encapsulated nattokinase polymeric nanoparticles are able to downregulate amyloid aggregation and exhibit antifibrinolytic activity. The encapsulation of nattokinase in PLGA did not affect its enzyme activity, so the prepared nanoformulation containing nattokinase can be used as an effective drug treatment against AD.

Keywords: nattokinase, PLGA, $A\beta_{40}$, Alzheimer's disease, surface modification, TEM, Tet1 peptide

Introduction

Alzheimer's disease (AD) is a serious neurodegenerative disease exemplified by the existence of hard plaques of Aβ inside the brain.[1] Its neurobehavioral outcomes include behavioral abnormality, dementia, social deterioration, and other cognitive dysfunctions. Physiologically, these senile plaques are extracellular in nature, and along with intracellular neurofibrillary tangles inside the brain cause atrophy of the neurons and synapses.[2,3] Globally by 2050, one in 85 people is predicted to be affected by AD. In the elderly, the prevalence of AD is highest (54%), followed by vascular dementia (34%). The probability of AD is higher in developing countries, due to the aging population. At present, 50% of people with AD are in developing countries, which is

likely to increase to 70% by 2025. In India, the prevalence of people with dementia is 33.6 per 1,000.[1]

Although accumulation of Aβ peptide is considered the trigger point for neuronal degeneration, the actual pathology of AD has not been well documented.[4,5] Aggregation of amyloid fibrils can induce cell death by disrupting cellular calcium ion-homeostasis.[6] Another pathology explaining AD is selective deposition of Aβ peptide in the mitochondria of cells, which inhibits uptake of glucose by neurons and key enzyme functions.[7,8] These days, an amyloid-cascade hypothesis is being used to try and modify and retard the progression of AD.

Nattokinase (NK; EC 3.4.21.62) is a powerful serine protease enzyme produced by *Bacillus subtilis* natto, and has been very popular due to its fibrinolytic activity. The molecular weight of NK is around 27.7 kDa, and it consist of 275 amino acids with a pI value of 8.6.[9–11] NK has been well studied for its cardiovascular activities, but its anti-AD effects have not been well studied so far. Few studies[12] have reported on the amyloid-degrading ability of NK during in vitro experimentation.[12,13] Therefore it could be a potential candidate if delivered at the site of Aβ accumulation by a targeted-delivery system. Although it has been proven that a decrease in fibrin and inflammation reduces the symptoms of AD,[14] NK has not been rigorously tested for AD. Apart from these findings, there is still no suitable formulation of NK for delivery into the brain.

The use of NK in the brain is very limited, because of its hydrophilic nature, stability issues, and lack of a delivery system that can address the limitation of protein formulations like aggregation, misfolding, and leakage during storage. A way to overcome these limitations could be nanoencapsulation of NK, helping it to cross the blood–brain barrier while retaining enzymatic activity.

To overcome these problems, the administration of polymeric NK nanoparticles (NPs) using a biopolymer like poly(lactic-*co*-glycolic acid) (PLGA) is one strategy by which aggregation and misfolding of the protein can be avoided. This confers stability by forming a shell around the protein in an organic solvent.[15] It also improves the pharmacokinetic properties of the protein.[16] Decreased immunogenicity is another benefit of such encapsulation.

PLGA is a well-established polymer with biocompatible and biodegradable properties. The US Food and Drug Administration and European Medicines Agency have approved PLGA for use as a polymer.[17] It can be metabolized easily inside the body via the Krebs cycle,[18] and its hydrolysis breaks it into glycolic acid and lactic acids. Various studies have reported the use of PLGA for polymeric NPs of anticancer drugs, nonsteroidal anti-inflammatory drugs, peptides, steroid hormones, and siRNA.[19,20] PLGA is used mainly for its sustained drug-release properties and site-directed delivery of compounds to specific tissue cells.[15]

The efficiency of a drug depends on its bioavailability at the site of action. Drug targeting to the brain has always been a challenge, due to the uncompromising character of the blood–brain barrier, limiting accessibility. The stringency of the blood–brain barrier is because the tight junctions at the capillary endothelium do not allow drugs through to the brain.[21] Various studies have reported employing PLGA for the development of brain targeting. There has been some success in synthesizing PLGA NPs (PNPs) of loperamide and conjugating them with glycosylated heptapeptides to specifically target the nervous system.[22]

With this background, we synthesized NK-PNPs (NKNPs) by employing a double-emulsion solvent-evaporation method and conjugated them with the Tet1 peptide, composed of 12 amino acids (HLNILSTLWKYR). This peptide has the ability for retrograde transport to neuronal cells and to interact with motor neurons, due to its affinity for them. Attachment of Tet1 peptide to NKNPs was done by adopting 1-ethyl-3-(3-dimethylaminopropyl)carbodiimide (EDC)–*N*-hydroxysuccinimide (NHS) coupling chemistry, which is widely used for surface modification and attachment of proteins to NPs.[23,24] The objective of this study was to report the formulation, optimization, and surface modification of NKNPs and to study their antiamyloid and antithrombotic potential for AD.

Materials and methods

NK (gift sample) was received from Zytex (Mumbai, India). Tet1 was custom-synthesized from GenPro Biotech (New Delhi, India). PLGA was received as a gift sample from Evonik (Essen, Germany). All chemicals used in the experimental studies were procured from Merck (Darmstadt, Germany). A Zetasizer Nano ZS (Malvern Instruments, Malvern, UK) was used for determination of polydispersity index (PDI) and particle size (PS) of the formulation. Transmission electron microscopy (TEM; CM-10; Philips, Amsterdam, the Netherlands) and scanning electron microscopy (SEM; Leo Electron Microscopy, Cambridge, UK) were used for the microscopic observation.

Formulation of NK-PLGA nanoformulation

Double-emulsification solvent evaporation was used to prepare the polymeric NK NPs.[23,25] PLGA was used as a polymer

to encapsulate NK. Tween 80 and Span 60 were used as emulsifiers in external and internal phases, and polyvinyl alcohol (PVA; 1%) was used as a stearic stabilizer. The first emulsion (W_1/O) was developed by dispersion of 150 µL NK of different concentrations (10%, 15%, and 20%) in 1.5 mL dichloromethane with PLGA (50–250 mg), Span 60 (10%–20% w:w solution), and Tween 80 (2.5%–15% w:w solution). This mixture was then subjected to sonication for 15 seconds at 50 W with a probe sonicator using an ice bath for temperature control, and the resulting primary emulsion was gradually deionized by addition of 5 mL PVA solution (1% w:v) premixed with Tween 80 (surfactant) in various concentrations (0.5%, 5%, 10%, and 15% w:v). This was followed by another round of sonication for 15 seconds under an ice bath to form a second emulsion ($W_1/O/W_2$). The emulsion obtained was then stirred constantly at 1,200 rpm under ambient temperature for 3 hours till the dichloromethane had completely evaporated. The developed NK NPs were harvested by five successive centrifugation cycles at 15,000 rpm for 30 minutes at 4°C. Washing and redispersion with deionized water were done to remove residual surfactants and free drug. The harvested NPs were again dispersed in a small volume of water and lyophilized to obtain powdered NPs. The final product was stored at −20°C until used for further characterization.

Optimization of formulation parameters using Box–Behnken design

The factors tested for NKNPs included NK-loading concentration (10%–20%), PLGA-polymer concentration (100–250 mg), sonication time (10–30 seconds), and concentrations of surfactants Span 60 (10%–20%) and Tween 80 (2.5%–7.5%). The effect of these factors on the formation of polymeric NPs was scrutinized statistically via response-surface methodology using Box–Behnken design (BBD) with Design Expert software 8.0.7.1. A three-level five-factor design of experiments was obtained for five independent factors from BBD with 46 runs (Table 1). Response-surface plots and their reciprocal contour plots were generated for better understanding of interaction between response variables and independent factors. Numerical and graphic optimizations were performed to finalize the optimum conditions for fabrication of the NK polymeric NPs.

PS and PDI

Dynamic light scattering was used for determination of PDI and PS using DTS Nano software.[26] PS and PDI were recorded by a 200-fold dilution of the formulation in the aqueous phase.[26]

TEM

Microscopic evaluation of optimized formulations was performed with TEM using the CM-10. TEM was performed as described in our previous study, with slight modifications.[38,39] A single drop of the developed NPs was kept over a carbon-coated grid along with phosphotungstic acid (2%), dried for 30 seconds, and covered with a coverslip. TEM observations were recorded operating at 60–80 kV.[26]

SEM

The optimized formulation was analyzed for its shape and surface morphology using SEM (S-3400N; Hitachi, Ltd., Tokyo, Japan) following the protocol of Bhatt et al.[38] The polymeric NPs were coated using gold sputter to make their surfaces more conductive.[26]

Encapsulation efficiency

The encapsulation efficiency (EE) of polymeric NK NPs was calculated from the difference between the initial amount of protein used to prepare NPs and the amount of protein present in supernatant after centrifugation at 15,000 *g* at 4°C for 30 minutes. The bicinchoninic acid protein assay was used for the quantification of protein. The following formula was used for the determination of EE and total amount of encapsulated NK:

$$\text{Quantity of encapsulated nattokinase} = \frac{\text{Total quantity of nattokinase}}{\text{Total quantity of nattokinase in supernatant}}$$

$$\text{Encapsulation efficiency} = \frac{\text{Total quantity of nattokinase encapsulated}}{\text{Total amount of nattokinase used for synthesis}} \times 100$$

Fourier-transform infrared spectroscopy

Fourier-transform infrared (FTIR) absorption spectra of the formulation were obtained with a an FTS-7000 (Varian, Palo Alto, CA, USA) using the disk technique (~5 mg) sample for 100 mg dry KBr. The KBr and formulation mixture was ground into fine powder and compressed into disk at a pressure of 10,000 psi and further analyzed using Win-IR software at wave numbers of 400–4,000 cm^{-1}.

Differential scanning calorimetry

A Pyris 6 (PerkinElmer, Waltham, MA, USA) was used for determination of thermal behavior of the NK nanoformulation and individual components as per Siddiqui et al, with minor modification.[27] In brief, 5–10 mg samples were

Table 1 Summary of experimental design, with actual and predicted values of dependent factors for NK polymeric NPs

Drug loading (%)	PLGA (mg)	Span 60 (%)	Tween 80 (%)	Sonication (seconds)	Particle size nm		PDI		EE (%)	
					Actual	Predicted	Actual	Predicted	Actual	Predicted
15	175	15	7.5	10	283	270.45	0.31	0.29	83	77.69
10	175	10	5	20	200	195.22	0.23	0.23	88.4	81.90
15	175	15	5	20	201	199.00	0.22	0.22	89.3	85.03
15	175	15	5	20	201	199.00	0.22	0.22	88.2	85.03
15	175	15	5	20	201	199.00	0.22	0.22	85.5	85.03
20	250	15	5	20	219.7	227.50	0.16	0.19	94.3	92.85
10	175	15	5	10	204	215.75	0.21	0.24	82.8	78.85
20	100	15	5	20	175	159.61	0.153	0.16	71.3	75.58
20	175	15	5	10	208	209.08	0.17	0.19	81.8	83.51
10	175	15	2.5	20	171	171.99	0.19	0.17	86.4	90.06
20	175	15	2.5	20	221.3	240.26	0.215	0.20	82.3	74.62
15	100	10	5	20	189.3	204.86	0.189	0.21	61.5	61.74
15	175	10	2.5	20	210	184.38	0.226	0.21	80.9	82.13
15	250	20	5	20	312	311.58	0.35	0.33	61	67.41
15	175	15	5	20	189	199.00	0.19	0.22	84.6	85.03
15	100	15	2.5	20	195.2	207.12	0.197	0.22	68.8	68.24
15	250	15	2.5	20	188	183.41	0.145	0.14	96.1	91.91
15	175	20	5	30	240.4	254.82	0.27	0.29	78.7	74.51
10	100	15	5	20	220.9	212.19	0.211	0.20	59.5	64.12
20	175	10	5	20	230.8	225.40	0.217	0.21	87.3	86.82
15	175	10	5	30	251	264.38	0.235	0.26	89.1	80.50
15	100	15	7.5	20	188	196.13	0.19	0.20	67.2	64.04
15	250	15	5	10	195	201.98	0.21	0.22	91.4	87.09
15	175	20	5	10	321	314.86	0.39	0.37	48.8	59.4
15	175	10	5	10	175	167.82	0.221	0.20	81.4	87.59
15	250	10	5	20	183.7	194.05	0.202	0.21	94.2	102.45
15	175	10	7.5	20	264	267.69	0.28	0.28	79.5	79.18
20	175	15	5	30	205	211.34	0.202	0.20	85.7	88.82
15	100	20	5	20	220	224.80	0.28	0.28	64.2	62.6
20	175	15	7.5	20	196.4	200.02	0.212	0.21	88.4	90.92
15	175	15	5	20	201	199.00	0.22	0.22	82.8	85.03
10	175	20	5	20	333.2	316.81	0.36	0.34	71.8	63.77
15	175	15	2.5	10	188.2	185.83	0.2	0.20	76.5	77.24
15	250	15	7.5	20	304.2	295.82	0.35	0.33	92.7	85.91
10	250	15	5	20	205.8	220.28	0.21	0.22	93.5	92.38
10	175	15	5	30	233	250.01	0.223	0.23	84.1	81.56
15	100	15	5	30	207	182.25	0.225	0.19	66.5	68.34
15	175	20	7.5	20	278.8	303.83	0.35	0.39	61.3	59.94
10	175	15	7.5	20	328	313.65	0.33	0.33	49.7	63.56
15	175	15	5	20	201	199.00	0.22	0.22	79.8	85.03
15	175	20	2.5	20	290	285.72	0.281	0.30	67	67.19
15	100	15	5	10	192.7	201.14	0.203	0.20	76.4	70.73
15	250	15	5	30	283.6	257.39	0.234	0.22	94.3	97.50
20	175	20	5	20	258.3	241.29	0.31	0.29	72.8	70.78
15	175	15	2.5	30	233	238.00	0.19	0.20	80.2	86.81
15	175	15	7.5	30	260	254.81	0.278	0.27	75.6	76.16

Note: Obtained from Box–Behnken design of response-surface methodology.
Abbreviations: NK, nattokinase; NPs, nanoparticles; PLGA, poly(lactic-*co*-glycolic acid); PDI, polydispersity index; EE, entrapment efficiency.

desiccated and kept inside aluminum pans that were then sealed, and a blank pan served as reference. Further, these pans were heated from 25°C to 450°C using a nitrogen atmosphere. The scanning rate for the samples was set at 10°C/min. The thermograms so obtained were evaluated to observe any changes in transition temperature of polymeric NPs, structural changes in PLGA after drug encapsulation, and possible interaction between NK and PLGA.

In vitro release

The release pattern of NK from NKNPs was observed by incubating them in PBS (pH 7) at 37°C for 36 hours. After 1,

6, 12, 24, and 36 hours, individual samples were taken by centrifugation at 15,000 *g* for 30 minutes at 4°C and supernatant replaced by fresh PBS. The amount of protein released was determined by bicinchoninic acid assay.[28]

Validation

Validation of the model for optimization of the polymeric NK NPs was carried out by comparing the experimentally determined values and predicted values of the responses using optimized preparation conditions as per BBD.

Surface modification

Conjugation of Tet1 with NKNPs was facilitated using EDC–NHS coupling chemistry as per Manish et al,[15] with minor modifications. Briefly, 100 µL NKNPs (~15 µg/mL) was activated using 100 mM NHS (200 µL) and 400 mM EDC (200 µL). This mixture was gently shaken and incubated for 1 hour at 37°C. After 1-hour incubation, 50 µL Tet1 (1 ng/mL) was added to the mixture, shaken well, and incubated for 12 hours with gentle shaking. After 12-hour incubation, conjugated NPs were collected by centrifugation at 10,000 rpm for 15 minutes at 4°C. The resultant NPs were washed twice with Milli-Q water and kept suspended in water for further analyses. Coupling of Tet1 with NKNPs was analyzed by attenuated total reflection (ATR)–FTIR spectroscopy.

Preparation of $A\beta_{40}$ fibrils

To evaluate the antiamyloid efficacy of the prepared NK-PGA nanoformulation, $A\beta_{40}$ plaques were developed as per Santin et al, with modification.[29] In brief, a stock solution of $A\beta_{40}$ (500 µM) was prepared in trifluoroethanol (75%). Peptide concentrations were quantified by recording absorbance at 275 nm. Fibrils were prepared by dilution of stock solution to 25 µM in 20 mM sodium PBS and 150 mM KCl (pH 7). The resultant solution was incubated at 25°C for 2 weeks. After 2 weeks, plaque formation was confirmed by SEM.

Thioflavin T-binding assay

The thioflavin T (ThT)-binding assay is based on the change in fluorescence intensity in ThT after binding with Aβ. Th stock solution (5 mM) was prepared in140 mM NaCl and 100 mM PBS with an adjusted pH of 8 and diluted to 200 µM concentration. Further, sample aliquots (30 µL) were mixed and incubated with ThT solution (30 µL of 200 µM) for 1 minute at 37°C and fluorescence intensity measured between 460 and 600 nm on an FP-750 spectrofluorometer (Jasco, Easton, MD, USA) with excitation at 442 nm.

In vitro amyloid degradation

After 2 weeks of $A\beta_{40}$-plaque formation, $A\beta_{40}$ plaques were treated with plain NK and different formulations to check the antiamyloid ability of the latter. Different formulations were incubated with a fixed volume of $A\beta_{40}$ plaques for 24 hours to 7 days, and then the digested plaques were observed under SEM.

In vitro thrombin plaque degradation

Fibrinolytic activity was assayed to estimate fibrinolytic activity of polymeric NK NPs with the method described in our previous study.[26] In brief, fibrinogen 0.72% (0.4 mL) was mixed with 250 mm phosphate buffer (pH 7, 0.1 mL) and incubated for 5 minutes at 37°C. Then, thrombin (0.1 mL, 20 U/mL) solution was added to this mixture and the solution = incubated for 10 minutes at 37°C. After incubation, a cloudy thrombin plaque was observed. To this, 0.1 mL enzyme solution/nanoformulation was added and further incubated. This solution was mixed at 20 minute intervals for 1 hour and 0.7 mL of 0.1 M trichloroacetic acid was added to stop enzyme activity. This reaction mixture was then centrifuged at 15,000 *g* for 10 minutes and absorbance measured at 275 nm. In this assay, one fibrinolytic unit of enzyme was defined as 0.01 increase per minute in absorbance of the reaction mixture. Images of the thrombin plaques were recorded before and after incubation with NKNPs and NPNP-Tet1.

Results

Formulation and optimization of NK-PLGA nanoformulation using BBD

Double-emulsion solvent evaporation was used to optimize polymeric NK NPs via using BBD. The effect of various independent factors, such as drug-loading concentration (5%–15%), PLGA-polymer concentration (150–200 mg), sonication time (10–30 seconds), and surfactant concentration on critical quality attributes (PS, PDI, EE) of polymeric NK NPs were investigated and are shown in Table 1.

NKNPs were prepared in 46 different batches as per the optimization design of BBD and analyzed for predicted and actual values of different independent factors (Table 1). After analysis of these 46 formulations, values of independent factors were optimized individually using the point-prediction tool of Design Expert. Using these optimized models, the experimental values of the responses were obtained: 163 nm PS, 0.1 PDI, 88% EE. Observed values were in close proximity with predicted values of responses, with low SD values.

The model for NPNP optimization was scrutinized and analyzed with Design Expert software, and actual and predicted values for the dependent factors (PS, PDI, and EE) presented resulted in the following quadratic equations:

$$PS = 199 + 11.3375 \times A + 18.99375 \times B + 34.36875 \times C + 25.35625 \times D + 9.13125 \times E + 14.95 \times AB 26.425 \times AC - 45.475 \times AD - 8 \times AE + 24.4 \times BC + 30.85 \times BD + 18.575 \times BE - 16.3 \times CD - 39.15 \times DE + 8.377 \times A^2 - 2.481 \times B^2 + 37.30 \times C^2 + 24.10 \times D^2 + 14.16 \times E^2$$

$$PDI = 0.215 - 0.20 \times A + 0.013 \times B + 0.049 \times C + 0.041 \times D - 0.0035 \times E + 0.002 \times AB - 0.009 \times AC - 0.035 \times AD + 0.0047 \times AE + 0.0142 \times BC + 0.053 \times BD + 0.0005 \times BE + 0.00375 \times CD - 0.0335 \times CE - 0.0055 \times DE - 0.0074 \times A^2 - 0.0152 \times B^2 + 0.0582 \times C^2 + 0.020 \times D^2 + 0.0065 \times E^2$$

$$EE = 85.033 + 2.98 \times A + 11.38 \times B - 8.54 \times C - 2.5 \times D + 2.006 \times E - 2.75 \times AB + 0.525 \times AC + 10.7 \times AD + 0.65 \times AE - 8.975 \times BC - 0.45 \times BD + 3.2 \times BE - 1.075 \times CD + 5.55 \times CE - 2.77 \times DE - 0.766 \times A^2 - 3.033 \times B^2 - 8.45 \times C^2 - 4.475 \times D^2 - 1.083 \times E^2$$

where A, B, C, D, and E are drug loading, polymer concentration, Span 60, Tween 80, and sonication time, respectively.

Surface plots (3-D response-surface and contour plots) were obtained by interaction between the two factors on the response, while keeping the other factor constant using Design Expert. 3-D response-surface and contour plots showing the effects of drug loading, polymer concentration, Span 60, Tween 80, sonication time, and effect of dependent variables (PS, PDI, and EE) in NK nanoformulation are presented in Figures 1–3 and Figures S1–S3. All three responses were positively influenced by five independent factors, and among these, two factors – drug loading and polymer concentration – showed higher values. The other three – sonication time and concentration of Span 60 and Tween 80 – favored lower or middle values.

From the 3-D surface and contour plots of PS (Figures 1 and S1), it can be deduced that interactions among polymer concentration, drug loading, and sonication time have an almost linear relationship. As the value of these three factors increased, larger PS and PDI were observed. Reduced interaction between drug loading and polymer concentration could be responsible for increased PS and PDI at extremities in the 3-D surface graph. The desired PS range and PDI value were obtained at the middle points of contour plots,

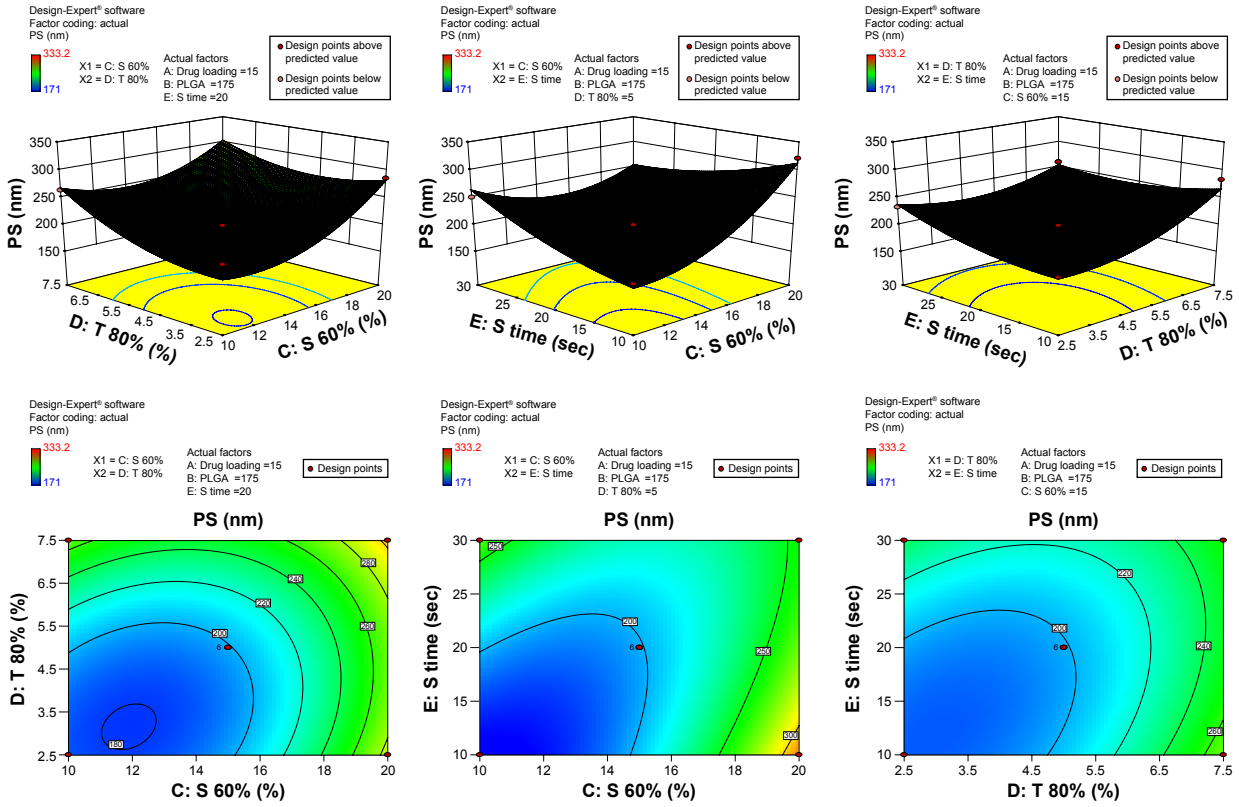

Figure 1 3-D surface and contour plots.
Note: Interaction effects of independent variables, such as drug loading, polymer concentration, sonication time, and concentration of surfactants, on particle size (PS).
Abbreviation: PLGA, poly(lactic-*co*-glycolic acid) nanoparticle.

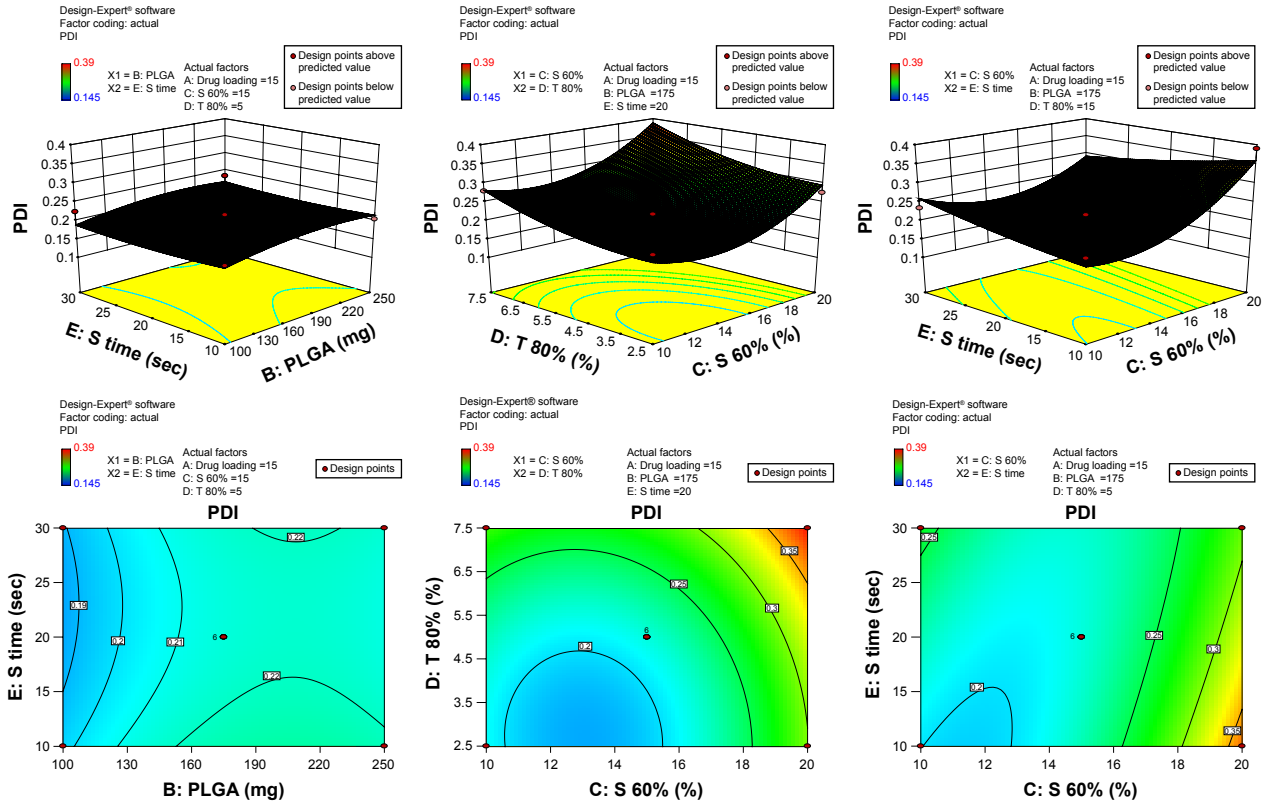

Figure 2 3-D surface and contour plots.
Note: Interaction effects of independent variables, such as drug loading, polymer concentration, sonication time, and concentration of surfactants, on polydispersity index (PDI).
Abbreviation: PLGA, poly(lactic-*co*-glycolic acid) nanoparticle.

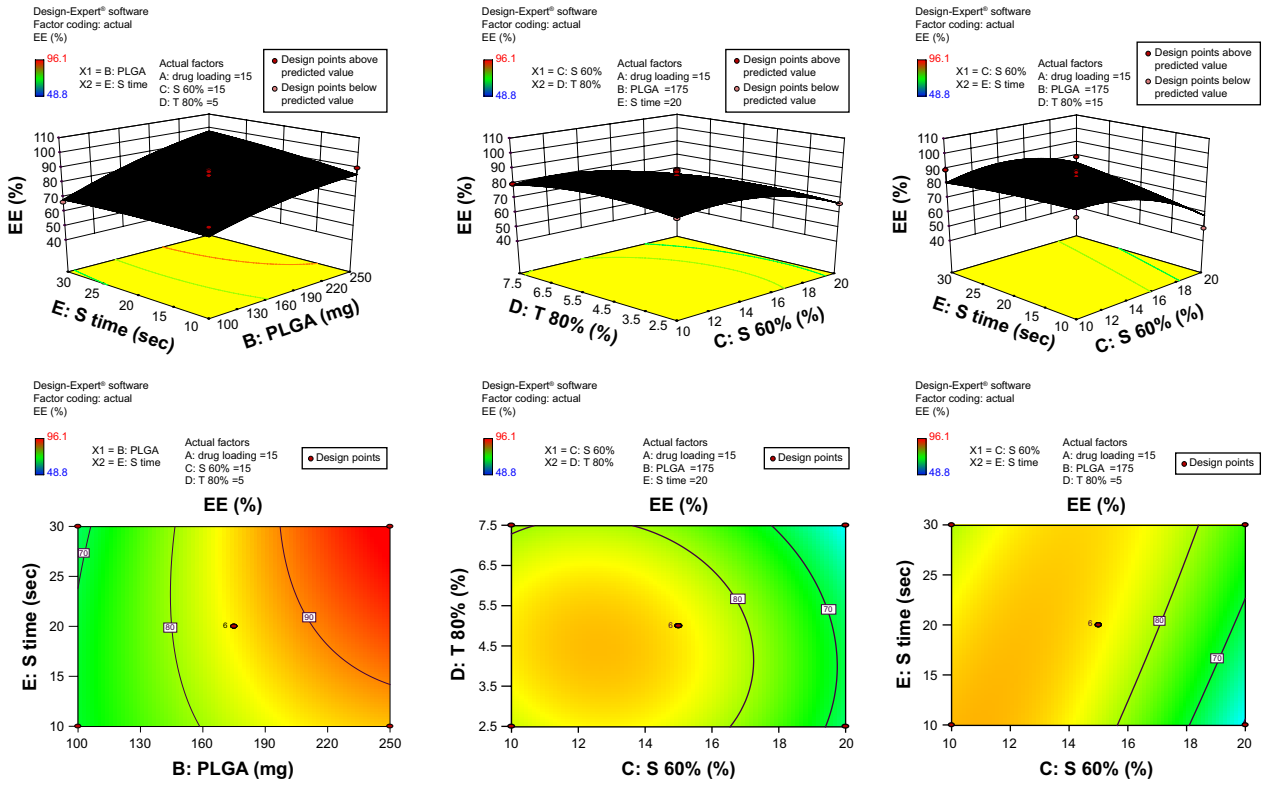

Figure 3 3-D surface and contour plots.
Note: Interaction effects of independent variables, such as drug loading, polymer concentration, sonication time and concentration of surfactants, on entrapment efficiency (EE).
Abbreviation: PLGA, poly(lactic-*co*-glycolic acid) nanoparticle.

yet increased to 320 nm and 0.36, respectively, at very low and high values (extremities of design) of independent variables.

The contour plot of EE (Figures 3 and S3) of polymeric NK NPs was significantly reduced after any change in independent variable beyond the middle point. The desired EE (>80%) of NKNPs was obtained at low–middle values of independent factors. Analysis of variance of PS, PDI, and EE is shown in Table 2. Point prediction was used to determine the optimum values of PS, PDI, and EE of NKNPs. Optimum values for drug loading (15%), polymer concentration (175 mg), Span 60 (10%), Tween 80 (2.5%), and sonication time (20 seconds) were obtained.

A model is considered significant if the significance probability value (*P*-value) is less than 0.05 (>95%). Analysis of variance revealed the significance ($P<0.05$) of the model. Table 2 shows that *F*- and lack-of-fit values for all responses were significantly affected by independent factors within the given range. Adequate precision, a measure of signal:noise ratio, was >4, which suggested that the model can be used to navigate the design space. Herein, all responses had adequate precision values >4 (Table 2), which indicated the efficiency and suitability of the present model to obtain the desired attributes.

Table 2 Analysis of variance of calculated model of NK polymeric NPs

Response	PS	PDI	EE (%)
Regression			
Sum of squares	83,080.36	0.1416	5,297.01
df	20	20	20
Mean squares	4,154.01	0.007	264.89
F-value	16.07	13.44	6.07
P-value	0.009	0.0001	0.0008
Residual			
Sum of squares	6,459.33	0.0131	1,089.17
df	25	25	25
Mean squares	258	0.0005	43.56
Lack-of-fit test			
Sum of squares	6,339.33	0.0124	1,028
df	20	20	20
Mean squares	316.96	0.00062	51.40
F-value	13.20	4.13	4.21
P-value	0.004	0.0608	0.0586
Coefficient correlation (r^2)	0.927	0.914	0.829
Coefficient of variation (%)	7.07	9.68	8.3
Adequate precision value	14.47	16.01	9.65
Predicted R^2	0.71	0.67	0.34
Adjusted R^2	0.87	0.84	0.69
SD	16.07	0.022	6.60
Mean	227.33	0.23	78.83

Abbreviations: NK, nattokinase; NPs, nanoparticles; PS, particle size; PDI, polydispersity index; EE, entrapment efficiency.

Validation of the model

Validation of the model for preparation of the polymeric NK NPs was carried out by comparing experimentally determined values and predicted values of responses using optimized preparation conditions as determined by BBD. Optimized independent factors showed 95%, 98%, and 110% validity for PS, PDI, and EE, respectively, for NKNPs. NPNP SEM revealed that particles were spherical with a distributive nature, as no aggregates were observed (Figure 4). TEM showed clear entrapment of drug in polymer when viewed at a scale of 0.1 μm, and particles of 100–200 nm were clearly observed (Figure 5). Optimal formulation conditions were significantly affected by the presence of NK, but at the same time, design space for the formulation was able to entrap the desired drug percentage. An entrapment efficiency of 88% was found to be optimal for the formulation.

PS and PDI

The PS of the optimized formulation was found to be 163 nm and the PDI value was 0.145 (Figure 6). Peak 1 signifies that the diameter of the particles with intensity 100% was 192.5 nm. The intensity of average PS was found to be 100%, which indicates that NKNPs had an intercept of 0.919. This confirmed that all particles in the formulation were uniform in size and distributed equally throughout the formulation. The PDI was found to be 0.145, signifying uniform distribution of the particles in the formulation. The average PS of the prepared NKNPs was found to be 161 nm and average particle width 80.4 nm with 192.5 nm diameter. Overall quality was assessed as good by DS Nano software (Figure 6).

TEM and SEM

The shape of the developed NPs was observed with TEM (Figure 5). Spherical NPs were observed with size in the nanometer range. Figure 5 shows a clear view of the entrapment of drug in polymer when viewed at a scale of 0.5 um. Particles of 140–160 nm were clearly observed. Figure 4 shows surface morphology and NP size and shape. The result shows that particles were spherical with smooth surfaces.

FTIR

FTIR spectra of NK, PLGA, and NKNPs are presented in Figure S4. Characteristic peaks for NK and PLGA were comparable with peaks of NKNPs. For PLGA, three peaks were observed, representing three stretches: 2,900–3,000 cm^{-1} represented C–H stretching of CH_3, while the other peak at 1,796 cm^{-1} represented carbonyl –C=O stretching and the

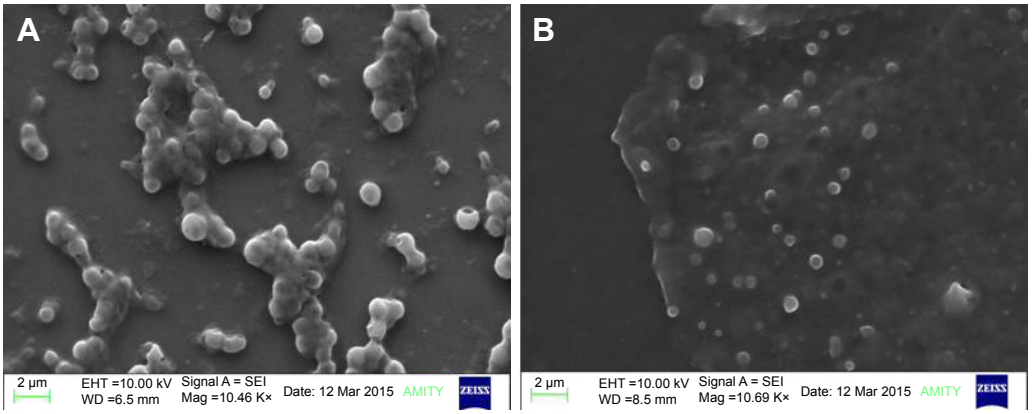

Figure 4 SEM of the optimized NPNP formulation at 10.46 K× (**A**) and 10.69 K× (**B**) magnification.
Abbreviations: SEM, scanning electron microscopy; NPNP, nattokinase–poly(lactic-*co*-glycolic acid) nanoparticle.

third peak at 1,090–1,179 cm^{-1} confirmed the presence of C–O stretching.

In NK spectra, three bands were observed that confirmed the presence of three amide bands (amide bands I, II, and III) with different stretching. The first signal was due to amide I, found at 1,641 cm^{-1} and representing C=O stretching, and the second signal was found at 1,531 cm^{-1} for the amide II band, representing N–H bending component and C–N stretching bands of the amide bond. The peak at 1,369 cm^{-1} signifies the presence of the amide III band. Typical C–H stretching (CH_3) at 2,866 cm^{-1} and CH_2 scissoring at 1,017 cm^{-1} were also observed.

The most significant signals of the amide I, II, and III bands (1,641, 1,531 and 1,369 cm^{-1}) of NK were clearly overlapped by the polymeric bands of NK-loaded NPs. In addition, NK-loaded particles showed specific functional groups of polymeric materials in NP surfaces with almost the same chemical characteristics as pure polymer. The entrapped drug did not show the expected main characteristic bands, because of the higher NK:polymer ratio in those particles. Furthermore, pure PLGA peaks (2,966 and 1,796 cm^{-1}) showed a small shift in NK-loaded particles (2,919 and 1,748 cm^{-1}) in comparison to the pure PLGA. In addition, the intensity of the absorption peak at 1,748 cm^{-1} was increased in NPs. Moreover, a small new peak at 2,919 cm^{-1} was observed in the NK-loaded particles. These observations suggest that NK was successfully loaded in the PLGA matrix.

Differential scanning calorimetry

Thermograms of NK and NK-loaded PLGA particles are shown in Figure S5. It was observed that NK exhibited a characteristic endothermic peak at 53°C, which could be attributed to absorbed water and melting point. This was

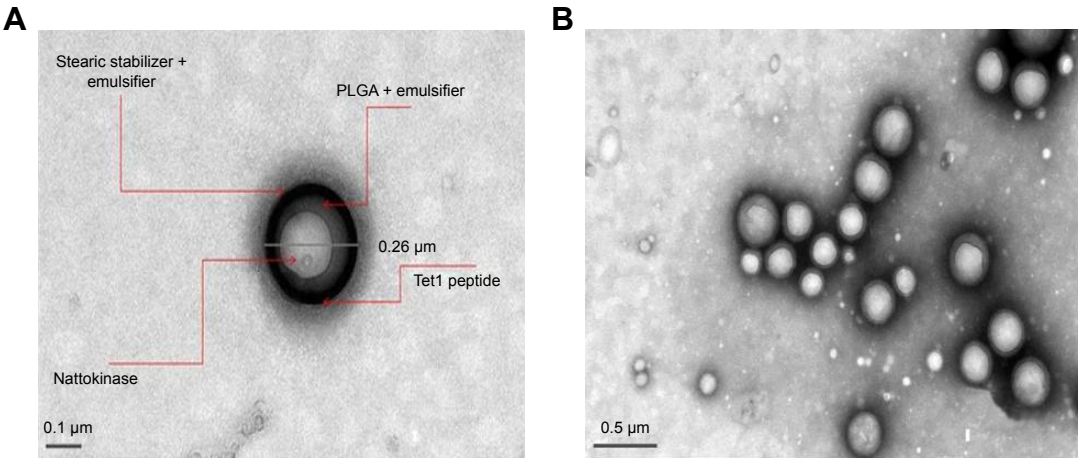

Figure 5 TEM of (**A**) conjugated and (**B**) optimized NPNP formulation.
Abbreviations: TEM, transmission electron microscopy; NPNP, nattokinase–poly(lactic-*co*-glycolic acid) nanoparticle; PLGA, poly(lactic-*co*-glycolic acid) nanoparticle.

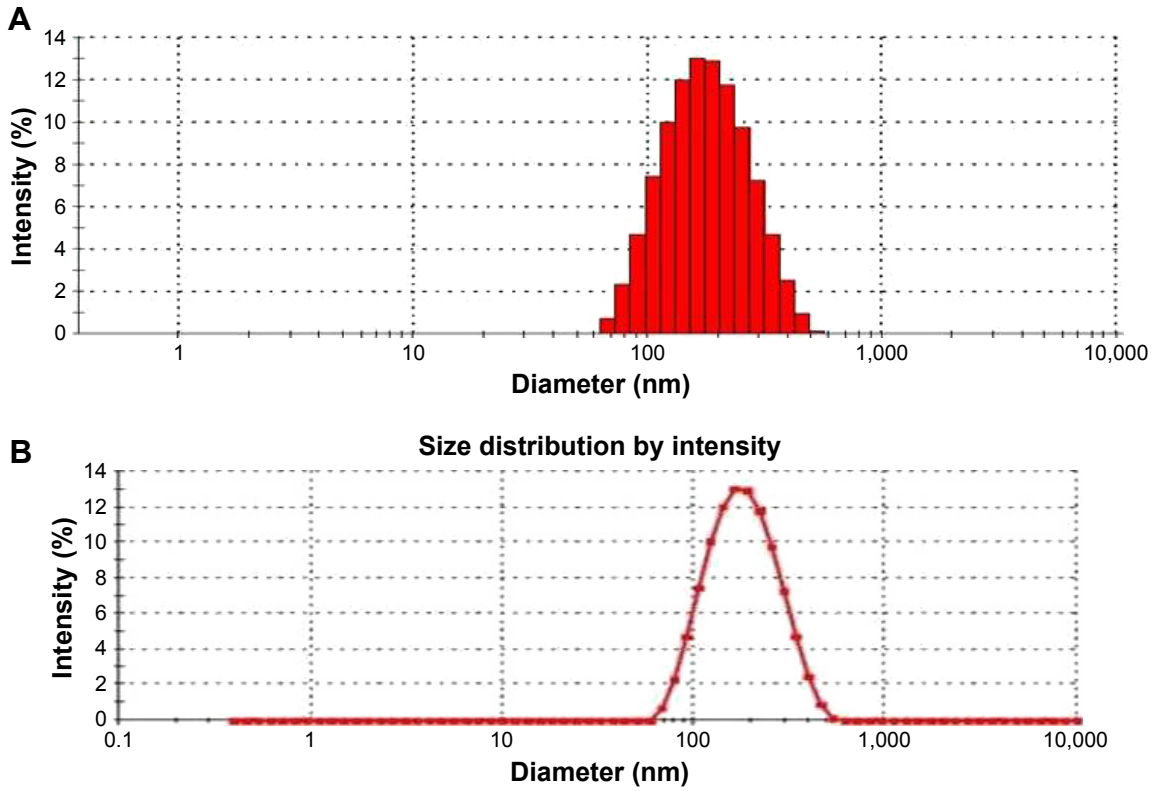

Figure 6 (**A**) Particle size and PDI of NKNPs; (**B**) particle-size distribution of NKNPs.
Abbreviations: PDI, polydispersity index; NKNPs, nattokinase–poly(lactic-*co*-glycolic acid) nanoparticles.

followed by conformational changes due to the unfolding of protein at 65°C. A bimodal peak starting at approximately 75°C–107°C was observed for NK-PLGA NPs. A significant shift in transition temperature (from 53°C to 107°C) of NK-PLGA NPs confirmed the molecular dispersion of NK inside the amorphous polymer matrix. These changes can be understood by the fact that NK exhibited its melting endothermic peak at 53°C, and any possible overlapping of this peak can result a change in its transition temperature. In our observation, there was no melting peak of NK found, which confirmed the complete encapsulation of NK inside PLGA.

In vitro release

The drug-release behavior of NKNPs was investigated, and it was observed that at the initial stage there was a relative drug-release burst followed by sustained release over 24 hours, with cumulative drug release of 80.23%±3.675% (n=3). The initial burst release can be correlated with a small part of the drug-enriched shell model. Most of the NK was encapsulated in the porous PLGA matrix, which resulted in prolonged release (Figure 7).

Surface modification

Surface modification of the NKNPs was done by conjugating Tet1 peptide onto NPNP surfaces. This conjugation of Tet1 with the nanoformulation was facilitated by employing an EDC-NHS reaction. Further, their attachment was confirmed by ATR-FTIR. ATR-FTIR analyses clearly indicated that there was no observable interaction between Tet1 and developed NKNPs. These observations also confirmed the conjugation of Tet1 onto the surfaces of NKNPs, as there

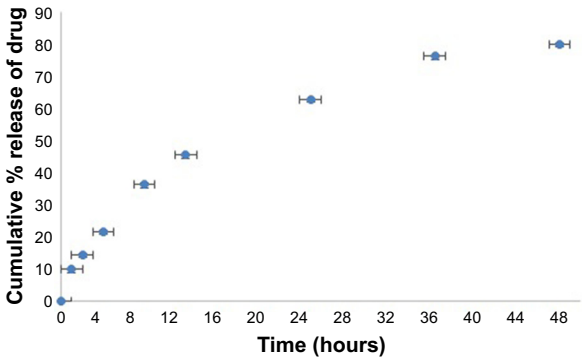

Figure 7 In vitro release of nattokinase from nattokinase polymeric nanoparticles at different time intervals (0–48 hours) using dialysis in PBS at pH 7.4.

were no additional peaks except the two major group peaks representing protein and peptide. Additionally, surface morphology of NPNP-Tet1 was investigated by TEM (Figure 5). The NPs were in moderate uniformity and spherical and smooth. The sphere volume of NPNP-Tet1 was slightly larger than NKNPs. The PS observed by TEM was in the nanometric range, as also observed by dynamic light scattering.

In vitro amyloid degradation on fluorescence

The amyloid-degrading activity of NKNPs was investigated on $A\beta_{40}$ plaques formed from synthetic $A\beta_{40}$ peptide. NK and NKNPs were both able to degrade the amyloid fibrils and were as effective as the pure NK. Figure 8 shows the ThT-binding assay, in which the intensity of ThT fluorescence at 487 nm suggested the loss of amyloid structure after digestion with NK and NKNPs. The results clearly revealed that NK and NKNPs and were able to degrade amyloid fibrils, and no alteration was observed in the enzymatic degradation of these plaques after nanoencapsulation.

In vitro amyloid degradation on SEM

Fibril morphology in amyloid plaques was studied under SEM before and after treatment with NKNPs. It was clearly observed that NKNPs and NPNP-Tet1 were able to degrade amyloid plaques completely (Figure 9), and there were no visible plaques after 24 hours of digestion. Both formulations were found to have the ability to digest the hard amyloid plaques completely.

In vitro thrombin plaque degradation

Free NK, NKNPs, and NPNP-Tet1 showed complete lysis of thrombin plaques (Figure 10). However, no lysis of thrombin plaque was observed in the absence of NK (control). No significant change in the in vitro thrombolytic activity of NK was found in NKNPs or NPNP-Tet1 before or after the preparation of NKNPs and surface modification. Nanoencapsulation of NK within PLGA and further surface modifications were able to retain all fibrinolytic activity (30 fibrinolytic units) under in vitro conditions.

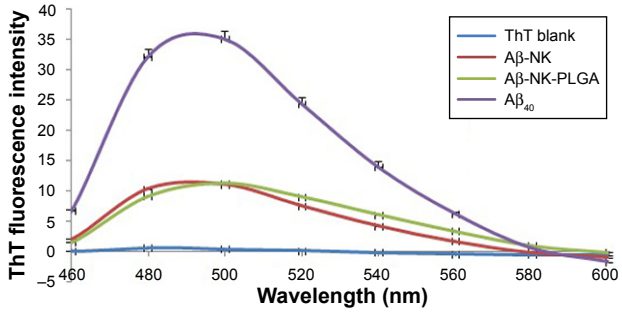

Figure 8 Fluorescence emission spectra obtained by using ThT binding assay of Aβ-40 plaque before (green line) and after digestion (24 hours) by nattokinase (red line) and NKNPs (blue line) and ThT was used as a blank (purple line) at 40°C, pH 7.
Abbreviations: ThT, thioflavin T; NK, nattokinase; PLGA, poly(lactic-*co*-glycolic acid); NKNPs, nattokinase–poly(lactic-*co*-glycolic acid) nanoparticles.

Discussion

There is an ever-growing demand for new foods or nutraceuticals that can provide therapeutic benefits to mankind. However, there are many troublesome challenges in the formulation of nutraceuticals, including development of a suitable delivery system, suitable formulation conditions, increased product shelf-life, increased bioavailability, prevention of therapeutic or nutraceutical activity degradation from heat, light, and oxidation, sensory properties of the product, prevention of active metabolites in the gastric environment, and transit. To overcome these challenges, nanoformulation of active metabolites can be a powerful strategy. Encapsulating nutraceutical metabolites or active ingredients from functional food inside a suitable polymeric matrix that can prevent degradation and control the release of the active moiety inside the biological system addresses the aforementioned challenges. The present investigation was such an attempt, where we attempted to develop an NK polymeric nanoformulation.

The aim of the current study was to fabricate and optimize a suitable drug-delivery system for NK and evaluate its potential for AD. Every aspect of the formulation development was studied extensively using different statistical combinatorial experimental designs for optimal formulation. Experimental conditions that yielded the best responses – mean PS <200 nm, PDI, and higher entrapment efficiency, along with desired morphology and shape of the particles – were optimized statistically by the BBD of response-surface methodology. By employing BBD, we investigated the effect of process (independent) variables on the quality attributes (dependent variables) of NPs. It was evident that all independent factors were necessary to obtain quality attributes of NKNPs and less than 10% of prediction errors were observed between the predicted and experimental values. This suggested that the model optimized by BBD was suitable for the preparation of polymeric NK NPs.

Double-emulsion solvent evaporation was used for the encapsulation of NK in PLGA. We explored the effect of different independent factors: Span 60 (in internal phase), Tween 80 (in external aqueous phase), PLGA concentration,

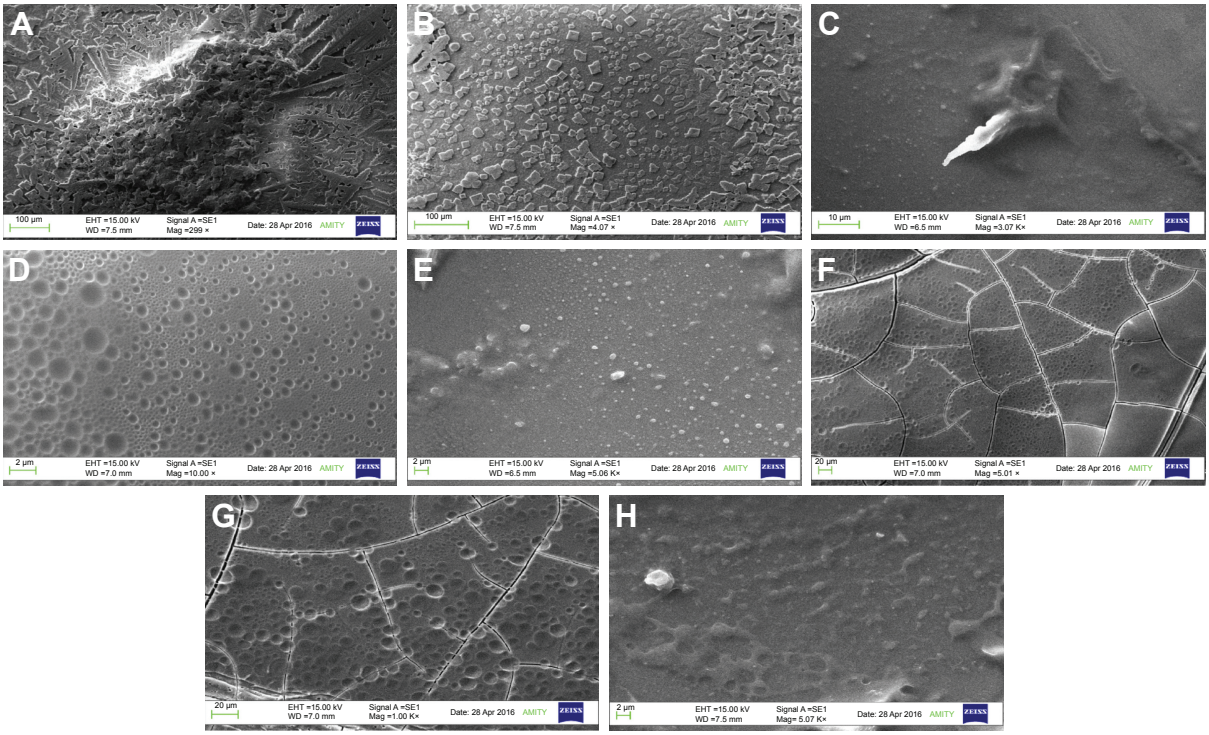

Figure 9 Scanning electron microscopy of $A\beta_{40}$ plaques.
Notes: Untreated $A\beta_{40}$ plaque (**A** and **B**), $A\beta_{40}$ plaques digested with unformulated nattokinase for 1 h (**C**), $A\beta_{40}$ plaques digested with unformulated nattokinase for 24 h (**D**), $A\beta_{40}$ plaques digested with NKNPs for 1 h (**E**) and for 24 h (**F**), $A\beta_{40}$ plaques digested with conjugated NKNPs for 1 h (**G**) and for 24 h (**H**).
Abbreviations: h, hours; NKNPs, nattokinase–poly(lactic-*co*-glycolic acid) nanoparticles.

sonication time, and drug-loading potential. Other parameters such as PVA, rate of stirring, and the volume ratio of primary and secondary emulsions (w/o/w), in both internal and external phases were kept constant.

Span 60 was selected as a surfactant emulsifier and added to the first emulsion because of its inherent property of enhancing stability of primary emulsions, as well as its drug-loading potential. Previous studies[15,16] have advocated

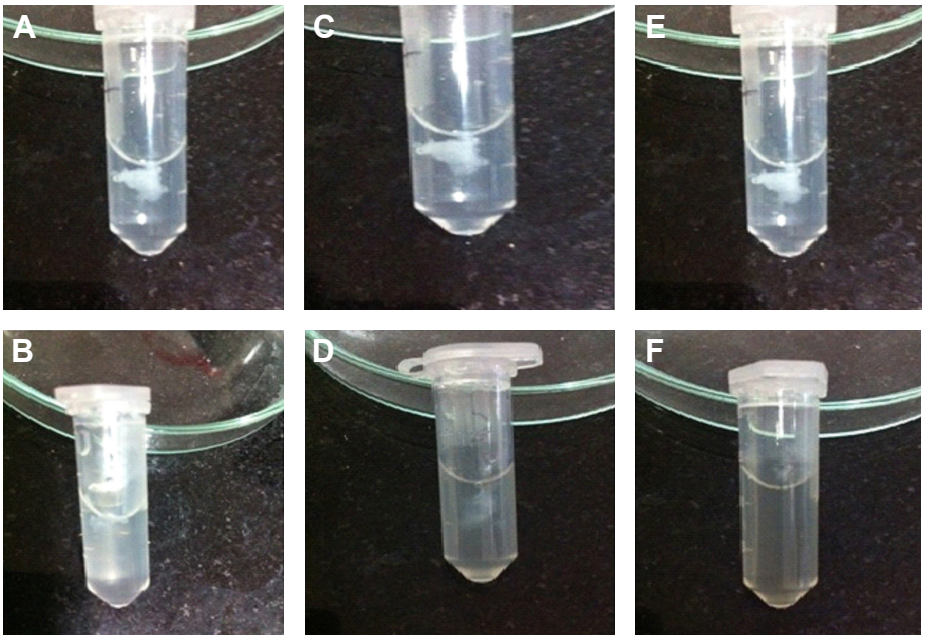

Figure 10 Invitro thrombin plaque inhibition of NK (**A** and **D**), NKNPs (**B** and **E**), and NKNPs-Tel-1 (**C** and **F**) before (**A**–**C**) and after (**D**–**F**) the preparation of NKNPs and surface modification.
Abbreviations: NK, nattokinase; NKNPs, nattokinase–poly(lactic-*co*-glycolic acid) nanoparticles.

that only a stable w/o emulsion can provide resistance for higher mass transfer. Therefore, drug molecules diffusing through the external phase would be reduced at the time of the second emulsification stage, which ultimately results in higher drug-loading efficiency.[30] As such, the high drug loading of NKNPs with strong mechanical strength to accommodate more than 80% of the drug can be attributed to Span 60 to a greater extent. Tween 80 was used as an emulsifier to the secondary emulsion because previous research[31] has advocated that with Tween 80 as an emulsifier, superior topographical characteristics within the resultant particles can be obtained.[19] These superior characteristics of our developed nanoformulation can be attributed to the better emulsification capabilities of Tween 80.

In double-emulsification and solvent evaporation, there was a continuous volume decrease during evaporation, as a result of which greater viscosity of the resultant emulsion was observed. This decrease in volume and increase in viscosity affected the droplet-size equilibrium, which consequently resulted in agglomeration of particles during solvent removal.[15,19] Coalescence and agglomeration of NPs can be avoided by the addition of PVA, which acts as a steric stabilizer in the continuous phase. PVA creates a protective layer (Figure 5), which helps the particles to stay apart and thus reduces their coalescence.[32]

During the formulation process, PVA binds to particle surfaces when the solvent evaporates from the interface and interpenetration occurs between the PVA and PLGA. Partially hydrolyzed PVA and its hydrophobic vinyl acetate part creates a binding site at the oil interface for binding with PLGA polymer during particle formation.[33,34] Therefore, it can be concluded that stearic stabilization is of utmost importance for formulation stability and prevention of coalescence and agglomeration.

Our study results clearly suggested that the physiochemical properties of the formulation were significantly influenced via formulating ingredients (Figures 1–3; Table 1). In most cases, second-order quadratic regression models were found to be adequate to describe the relationship between different formulation ingredients and their effect on formulation parameters ($R^2 > 0.927$). The quadratic effects of polymer, surfactant, emulsifier concentration, drug, and sonication time had significant ($P < 0.0001$) effects on all response variables studied.

PS is a significant parameter that estimates the fate of NPs.[19] It has been established by earlier studies[15] that nanocarriers of 100–200 nm are known to have better release properties. Our results were in agreement with previous studies, and substantiate the fact that smaller particles exhibit better release properties. In this contribution, a five-factor statistical experimental design was used for the optimization of different independent factors using PS, PDI, and EE as their dependent factors. Under the optimized condition, the mean diameter of NKNPs was found to be in the nanometric range. It has been observed that an increase in drug also increases NP PDI.[17] In this study, NKNPs exhibited narrow particle distribution (PDI <0.1),[20] which indicated that nice encapsulation of NK was achieved.

Formation of amyloid plaques has been considered one of the main pathological outcomes of AD, and similarly $A\beta_{40}$ has been the major breakdown product of amyloid-precursor protein, as well as the main component in amyloid plaques. As a result, we evaluated the prepared nanoformulation for its ability to disintegrate amyloid plaques developed under in vitro conditions using $A\beta_{40}$. Study results revealed that the developed nanoformulation was able to disintegrate the amyloid plaque completely. The PLGA-encapsulated NK NPs conserved the antiamyloid property and were able to disintegrate Aβ plaques. Surface modification by attachment of Tet1 to the NPs did not affect antiamyloid or fibrinolytic activity.

We were able to reproduce the amyloid-degrading activity shown by raw NK in our PLGA-encapsulated NK NPs. The NK NPs were able to stop the aggregation of amyloid plaques and disrupt the aggregates that were already formed. Our results were in agreement with the previous research,[35] and substantiates the amyloid-degrading ability of NK. It has been reported that NK also has the capacity to decrease Aβ by decreasing fibrin content in the blood and its leakage in the brain, thus indirectly inhibiting plaque formation.[36] Delivery of the drug to the right target has been equally important as the drug's own activity. Because of the stringent nature of the blood–brain barrier, it has been a challenge to target cerebral disease with specific drugs. The blood–brain barrier has been known to prevent the entry of any particle into the brain. Being a hydrophilic protein, NK is unable enter the brain by directly crossing the blood–brain barrier. By encapsulating NK into the PLGA matrix, it was modified in such a way that it gained the ability to cross the blood–brain barrier. Combining NPs with Tet1 could be one potential strategy to increase the uptake of NPs by neuronal cells. Previous research has adopted similar strategies to combine PLGA NPs with glycosylated heptapeptide for brain targeting. Recently, one research group was successful in brain targeting using a peptide conjugated with PEG-PLGA NPs, and the study also reported the movement of particles inside the brain crossing the blood–brain barrier when studied under in vivo

conditions. By taking a clue from these studies, we evaluated NKNPs developed against amyloid plaques under in vitro conditions, in order to justify the proposed therapeutic use against AD. Our findings were in agreement with previously reported work,[37] which had already suggested that NK significantly degrades amyloid plaques. The antiamyloid effect of NKNPs can be conferred upon their proteolytic, antifibrinolytic, and antithrombotic actions; therefore, it is suggested that NKNPs may be an effective treatment for prevention and treatment of AD.

A delivery system that includes the encapsulation of the hydrophilic protein NK into biocompatible and biodegradable polymer PLGA was developed, and it was observed that other formulation ingredients had a significant effect on the stability of the final product. High-molecular-weight PVA acts as a stearic stabilizer, provides the most significant stability, and prevents drug leakage from NPs. It can be concluded that a stearic stabilization is of utmost important for hydrophilic protein drug encapsulation. FTIR analysis clearly indicated that there was no significant interaction between the active protein drug and formulation ingredients.

Although our primary objective in this study was to develop a nanodelivery system for NK and surface engineering for the attachment of Tet1 using EDC-NHS coupling chemistry, at the same time it is of utmost importance that the developed system should have a therapeutic target, so we tested the developed nanoformulation against Aβ and fibrin plaques. Here, we have reported a nanoencapsulation followed by surface modification of NK with Tet1. Earlier, we studied the fibrinolytic activity of an NK nanoformulation[28] and validated the well-established fibrinolytic activity of NK. Further in vitro work by Hsu et al advocated the anti-AD activity of NK.[12] Taking a clue from these studies, it can be postulated that NK has the dual potential of degrading fibrin as well as Aβ.[12,28] Along with these dual-inhibitory properties, NK can be used to prevent the joining of fibrin with Aβ and thus prevent clot formation inside the brain.

Apart from this evidence, in our study surface modification was performed to conjugate polymeric NK NPs with Tet1, which is composed of 12 amino acids (HLNILSTLWKYR) and has the ability of retrograde transport to the neuronal cells and to interact with motor neurons, due to its affinity for them. Therefore, direct Aβ targeting inside the brain can be achieved by Tet1-guided delivery of NK to the target site. Taken together, all these activities of NK and NKNPs strongly point to anti-AD activity; therefore, the possibility of NK as a potential candidate for AD treatment cannot be ruled out.

Conclusion

Any treatment formulated for AD should be designed in such a way that it addresses the multifactorial etiologies of the disease. It is a well-established fact that other than amyloid plaques, there are various other factors, such as cholesterol homeostasis, that play a crucial role in the progression of the disease. An NK nanoformulation with various therapeutic benefits could be a potential drug in treating AD. The present study has suggested that Tet1-conjugated NKNPs can be potential candidates in treating AD, due to their antiamyloid and antifibrinolytic activities.

The biocompatible nature of NK and a vast history of its medicinal use, along with lower cost of production, favors its commercialization as a nutraceutical candidate for prevention and treatment of AD. In a continuation of this work, our research group is studying NKNPs in two different animal models of AD to validate the in vitro results further, which could further suggest that NK can offer neuroprotection from amyloid plaque-induced neuronal damage. In conclusion, development of NK using a US Food and Drug Administration-approved polymer, such as PLGA, with higher drug-entrapment efficiency and desired release properties has paved the way for development of novel drug-delivery systems for therapeutic proteins from functional foods and nutraceuticals.

Acknowledgment

The authors acknowledge the grant (SB/FT/LS-316/2012) received from the Science and Engineering Research Board, Department of Science and Technology, Government of India under the DST Fast Track Scheme.

Disclosure

The authors report no conflicts of interest in this work.

References

1. Alzheimer's Association. 2013 Alzheimer's disease facts and figures. *Alzheimers Dement*. 2013;9(2):208–245.
2. Cummings JL. Alzheimer's disease. *N Engl J Med*. 2004;351:56–67.
3. Mucke L. Alzheimer's disease. *Nature*. 2009;461:895–897.
4. McDonald B, Esiri MM, Morris J. Aluminium and Alzheimer's disease. *Age Ageing*. 1993;22:392–393.
5. Vemuri P, Lesnick TG, Przybelski SA, et al. Age, Vascular Health, and Alzheimer's disease Biomarkers in an Elderly Sample. *Ann Neurol*. Epub 2017 Oct 10.
6. Lu JX, Qiang W, Yau WM, Schwieters CD, Meredith SC, Tycko R. Molecular structure of β-amyloid fibrils in Alzheimer's disease brain tissue. *Cell*. 2013;154:1257–1268.
7. Fändrich M. On the structural definition of amyloid fibrils and other polypeptide aggregates. *Cell Mol Life Sci*. 2007;64:2066–2078.
8. Serpell LC. Alzheimer's amyloid fibrils: structure and assembly. *Biochim Biophys Acta*. 2000;1502:16–30.

9. Liang X, Zhang L, Zhong J, Huan L. Secretory expression of a heterologous nattokinase in *Lactococcus lactis*. *Appl Microbiol Biotechnol*. 2007;75:95–101.
10. Dubey R, Kumar J, Agrawala D, Char T, Pusp P. Isolation, production, purification, assay and characterization of fibrinolytic enzymes (nattokinase, streptokinase and urokinase) from bacterial sources. *Afr J Biotechnol*. 2011;10:1408–1420.
11. Cho YH, Song JY, Kim KM, et al. Production of nattokinase by batch and fed-batch culture of *Bacillus subtilis*. *N Biotechnol*. 2010;27:341–346.
12. Hsu RL, Lee KT, Wang JH, Lee LY, Chen RP. Amyloid-degrading ability of nattokinase from *Bacillus subtilis* natto. *J Agric Food Chem*. 2009;57:503–508.
13. Wang C, Du M, Zheng D, Kong F, Zu G, Feng Y. Purification and characterization of nattokinase from Bacillus subtilis natto B-12. *J Agric Food Chem*. 2009;57:9722–9729.
14. Akiyama H, Barger S, Barnum S, et al. Inflammation and Alzheimer's disease. *Neurobiol Aging*. 2000;21:383–421.
15. Manish M, Bhatnagar R, Singh S. Preparation and characterization of PLGA encapsulated protective antigen domain 4 nanoformulation. *Methods Mol Biol*. 2016;1404:669–681.
16. Manish M, Rahi A, Kaur M, Bhatnagar R, Singh S. A single-dose PLGA encapsulated protective antigen domain 4 nanoformulation protects mice against *Bacillus anthracis* spore challenge. *PLoS One*. 2013;8:e61885.
17. Tao W, Zeng X, Liu T, et al. Docetaxel-loaded nanoparticles based on star-shaped mannitol-core PLGA-TPGS diblock copolymer for breast cancer therapy. *Acta Biomater*. 2013;9:8910–8920.
18. Idelchik GM, Varon J. Hypocarbia, therapeutic hypothermia, and mortality: the Kreb cycle is key. *Am J Emerg Med*. 2014;32:643–644.
19. Jagani HV, Josyula VR, Palanimuthu VR, Hariharapura RC, Gang SS. Improvement of therapeutic efficacy of PLGA nanoformulation of siRNA targeting anti-apoptotic Bcl-2 through chitosan coating. *Eur J Pharm Sci*. 2013;48:611–618.
20. Verderio P, Bonetti P, Colombo M, Pandolfi L, Prosperi D. Intracellular drug release from curcumin-loaded PLGA nanoparticles induces G2/M block in breast cancer cells. *Biomacromolecules*. 2013;14:672–682.
21. Kumar PV, Bhopal AK. Formulation design and evalution of rutin loaded selfemulsifying drug delivary [sic] system (SEDDs) using edible oil. *Asian J Pharm Clin Res*. 2012;5:76–78.
22. Saxton WM, Hollenbeck PJ. The axonal transport of mitochondria. *J Cell Sci*. 2012;125:2095–2104.
23. Makadia HK, Siegel SJ. Poly lactic-*co*-glycolic acid (PLGA) as biodegradable controlled drug delivery carrier. *Polymers (Basel)*. 2011;3:1377–1397.
24. Danhier F, Ansorena E, Silva JM, Coco R, Le Breton A, Préat V. PLGA-based nanoparticles: an overview of biomedical applications. *J Control Release*. 2012;161:505–522.
25. Lee JY, Bashur CA, Goldstein AS, Schmidt CE. Polypyrrole-coated electrospun PLGA nanofibers for neural tissue applications. *Biomaterials*. 2009;30:4325–4335.
26. Bhatt PC, Srivastava P, Pandey P, Khan W, Panda BP. Nose to brain delivery of astaxanthin-loaded solid lipid nanoparticles: fabrication, radio labeling, optimization and biological studies. *RSC Adv*. 2016;6(12):10001–10010.
27. Siddiqui IA, Sanna V, Ahmad N, Sechi M, Mukhtar H. Resveratrol nanoformulation for cancer prevention and therapy. *Ann N Y Acad Sci*. 2015;1348:20–31.
28. Kapoor R, Harde H, Jain S, Panda AK, Panda BP. Downstream processing, formulation development and antithrombotic evaluation of microbial nattokinase. *J Biomed Nanotechnol*. 2015;11:1213–1224.
29. Santin MD, Vandenberghe ME, Herard AS, et al. In vivo detection of amyloid plaques by gadolinium-stained MRI can be used to demonstrate the efficacy of an anti-amyloid immunotherapy. *Front Aging Neurosci*. 2016;8:55.
30. Arora S, Swaminathan SK, Kirtane A, et al. Synthesis, characterization, and evaluation of poly (D,L-lactide-*co*-glycolide)-based nanoformulation of miRNA-150: potential implications for pancreatic cancer therapy. *Int J Nanomedicine*. 2014;9:2933–2942.
31. Zhang Z, Feng SS. In vitro investigation on poly(lactide)-Tween 80 copolymer nanoparticles fabricated by dialysis method for chemotherapy. *Biomacromolecules*. 2006;7:1139–1146.
32. Milacic VM, Schwendeman SP. Lysozyme release and polymer erosion behavior of injectable implants prepared from PLGA-PEG block copolymers and PLGA/PLGA-PEG blends. *Pharm Res*. 2014;31:436–448.
33. Niu C, Graves JD, Mokuolu FO, Gilbert SE, Gilbert ES. Enhanced swarming of bacteria on agar plates containing the surfactant Tween 80. *J Microbiol Methods*. 2005;62:129–132.
34. Beletsi A, Panagi Z, Avgoustakis K. Biodistribution properties of nanoparticles based on mixtures of PLGA with PLGA-PEG diblock copolymers. *Int J Pharm*. 2005;298:233–241.
35. Chen PT, Chiang CJ, Chao YP. Strategy to approach stable production of recombinant nattokinase in *Bacillus subtilis*. *Biotechnol Prog*. 2007;23:808–813.
36. Wang SL, Chen HJ, Liang TW, Lin YD. A novel nattokinase produced by *Pseudomonas* sp. TKU015 using shrimp shells as substrate. *Process Biochem*. 2009;44:70–76.
37. Balasubramanian S, Girija AR, Nagaoka Y. Curcumin and 5-fluorouracil-loaded, folate- and transferrin-decorated polymeric magnetic nanoformulation: a synergistic cancer therapeutic approach, accelerated by magnetic hyperthermia. *Int J Nanomedicine*. 2014;9:437–459.
38. Bhatt PC, Pathak S, Kumar V, Panda BP. Attenuation of neurobehavioral and neurochemical abnormalities in animal model of cognitive deficits of Alzheimer's disease by fermented soybean nanonutraceutical. *Inflammopharmacol*. Epub 2017 Aug 8.
39. Kumar V, Bhatt PC, Rahman M, et al. Fabrication, optimization, and characterization of umbelliferone β-D-galactopyranoside-loaded PLGA nanoparticles in treatment of hepatocellular carcinoma: in vitro and in vivo studies. *Int J Nanomedicine*. 2017;12:6747–6758.

Supplementary materials

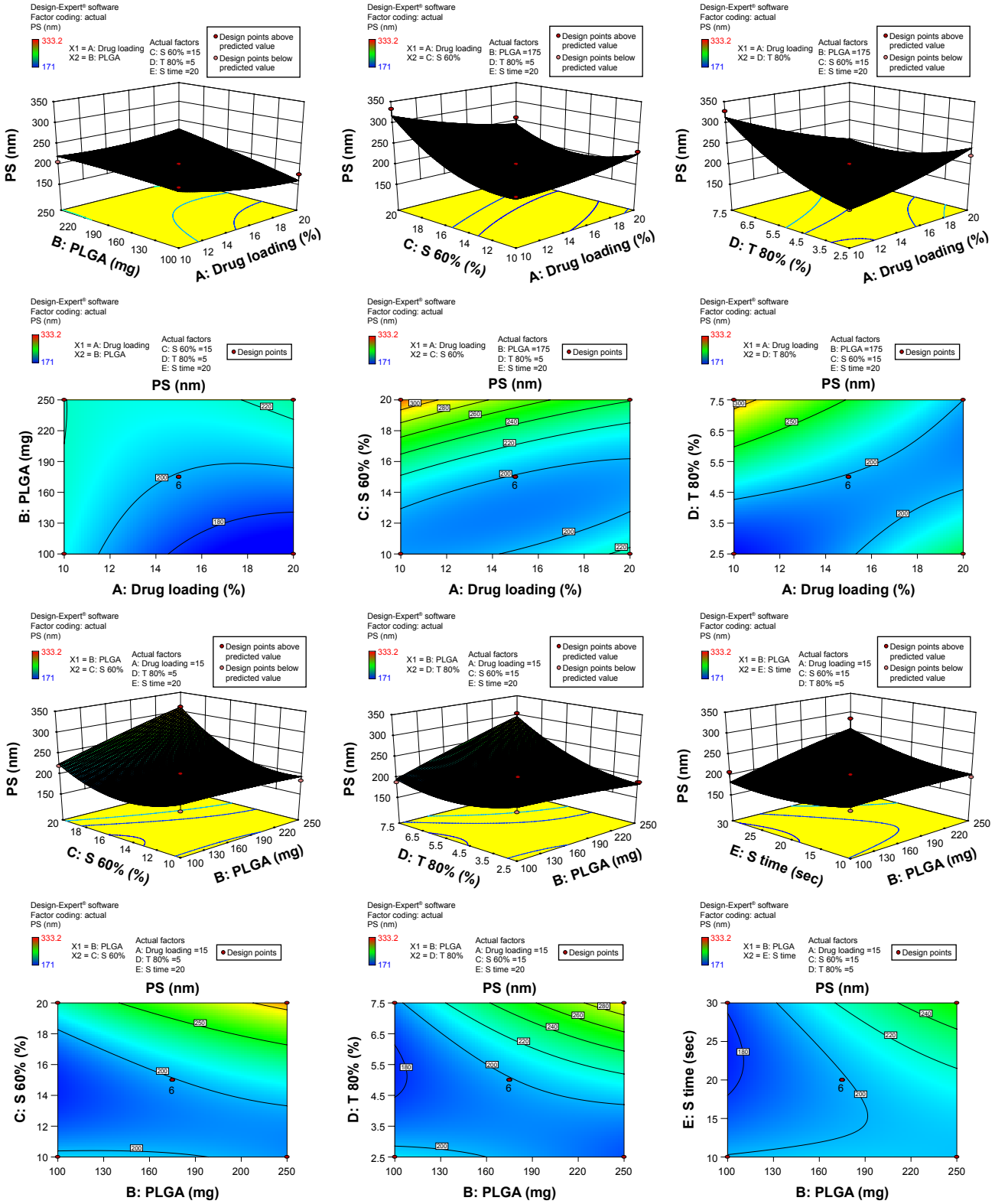

Figure S1 3-D surface and contour plots.
Note: Interaction effects of independent variables, such as drug loading, polymer concentration, sonication time, and concentration of surfactants, on particle size (PS).
Abbreviation: PLGA, poly(lactic-*co*-glycolic acid) nanoparticle.

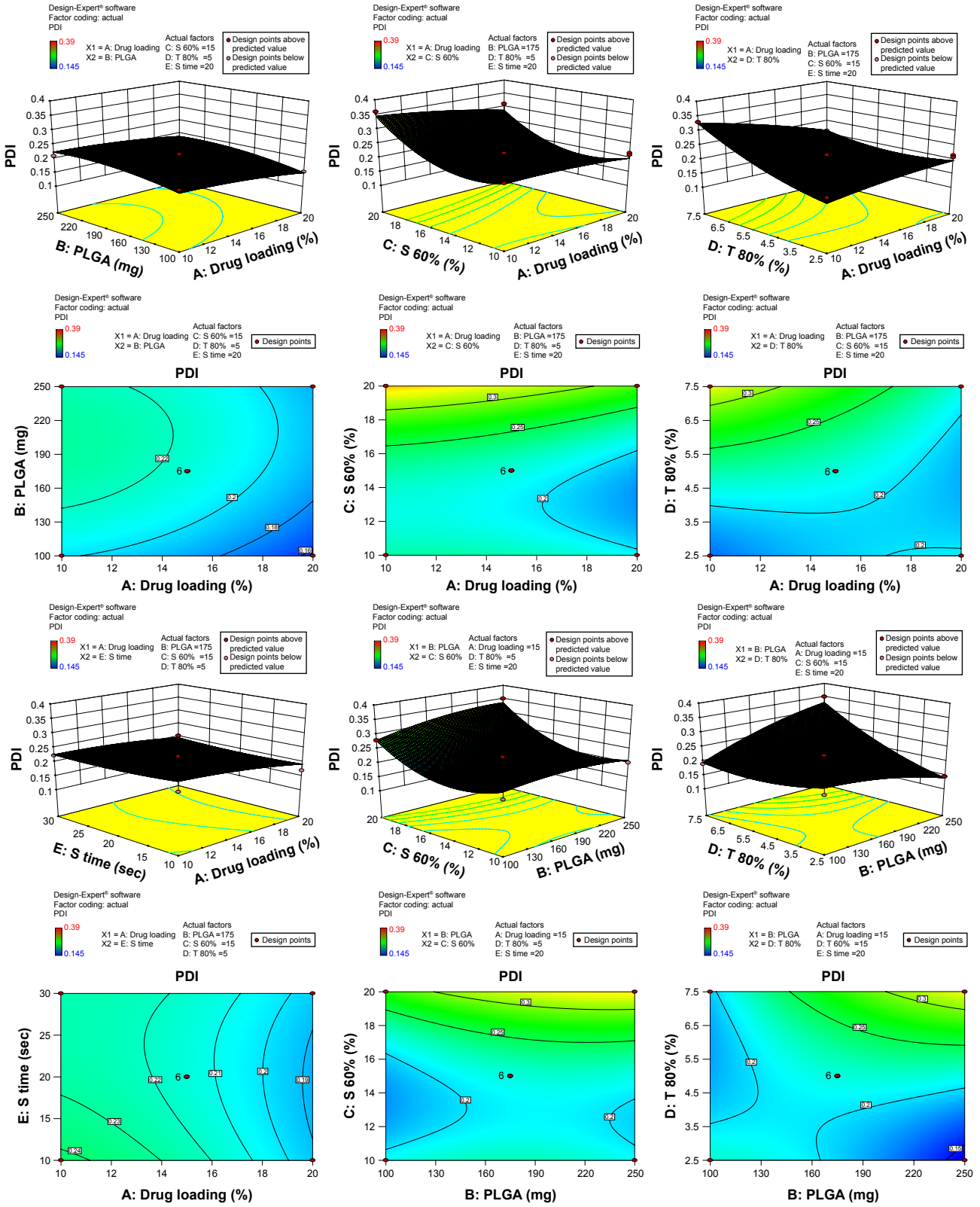

Figure S2 3-D surface and contour plots.
Note: Interaction effects of independent variables, such as drug loading, polymer concentration, sonication time, and concentration of surfactants, on polydispersity index (PDI).
Abbreviation: PLGA, poly(lactic-*co*-glycolic acid) nanoparticle.

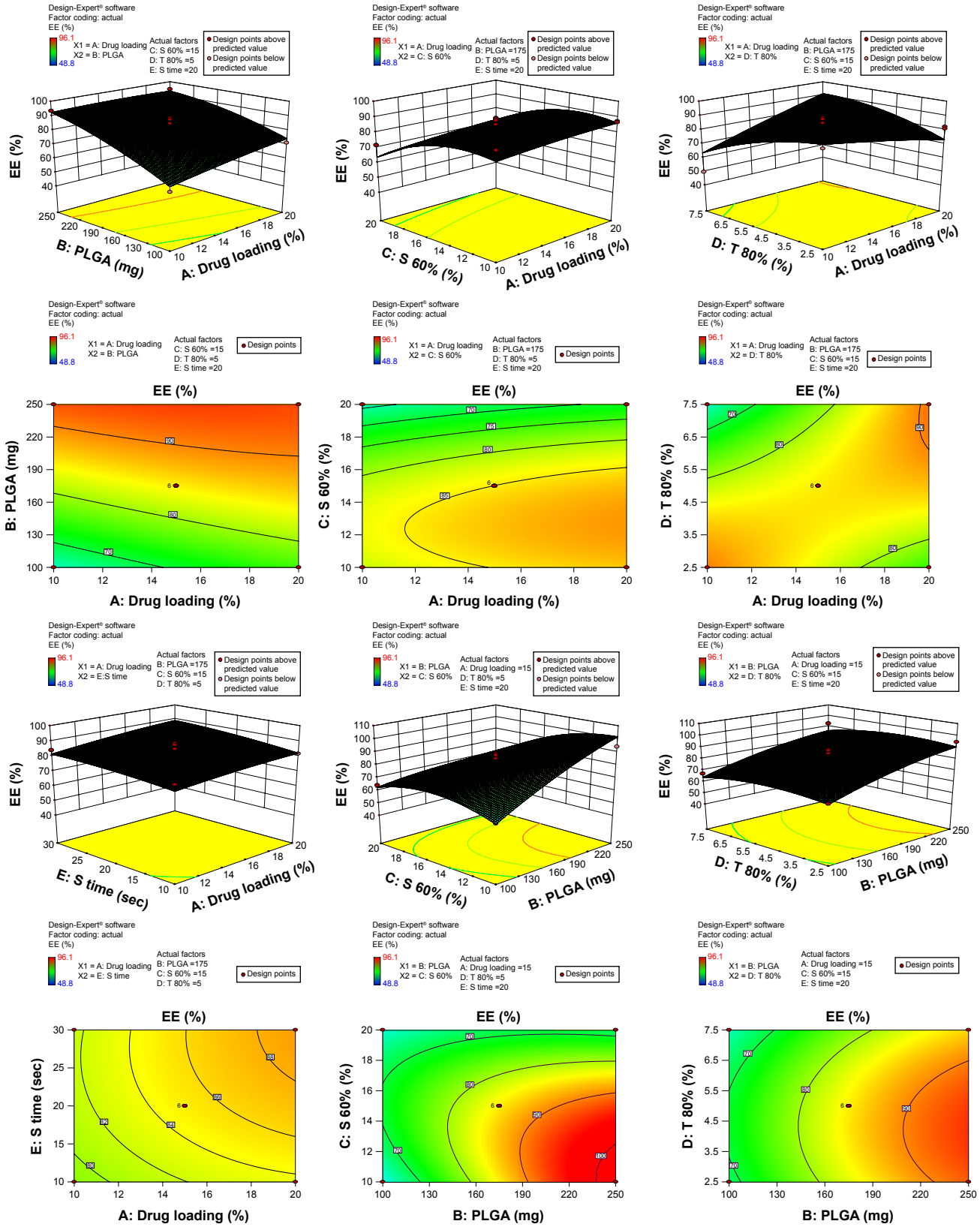

Figure S3 3-D surface and contour plots.

Note: Interaction effects of independent variables, such as drug loading, polymer concentration, sonication time, and concentration of surfactants, on entrapment efficiency (EE).

Abbreviation: PLGA, poly(lactic-*co*-glycolic acid) nanoparticle.

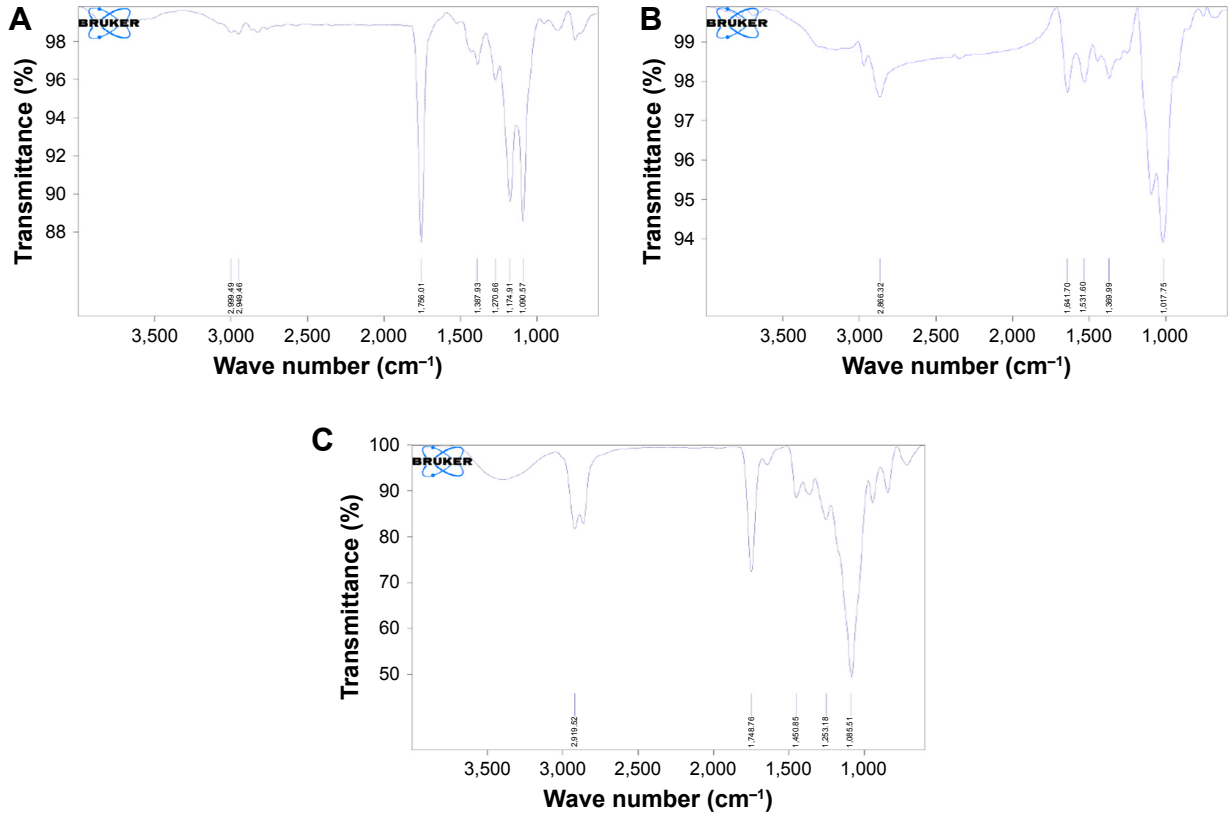

Figure S4 FTIR spectra of (**A**) PLGA polymer, (**B**) NK, and (**C**) NKNPs.
Abbreviations: FTIR, Fourier-transform infrared; NK, nattokinase; PLGA, poly(lactic-*co*-glycolic acid); NKNPs, NK-PLGA nanoparticles.

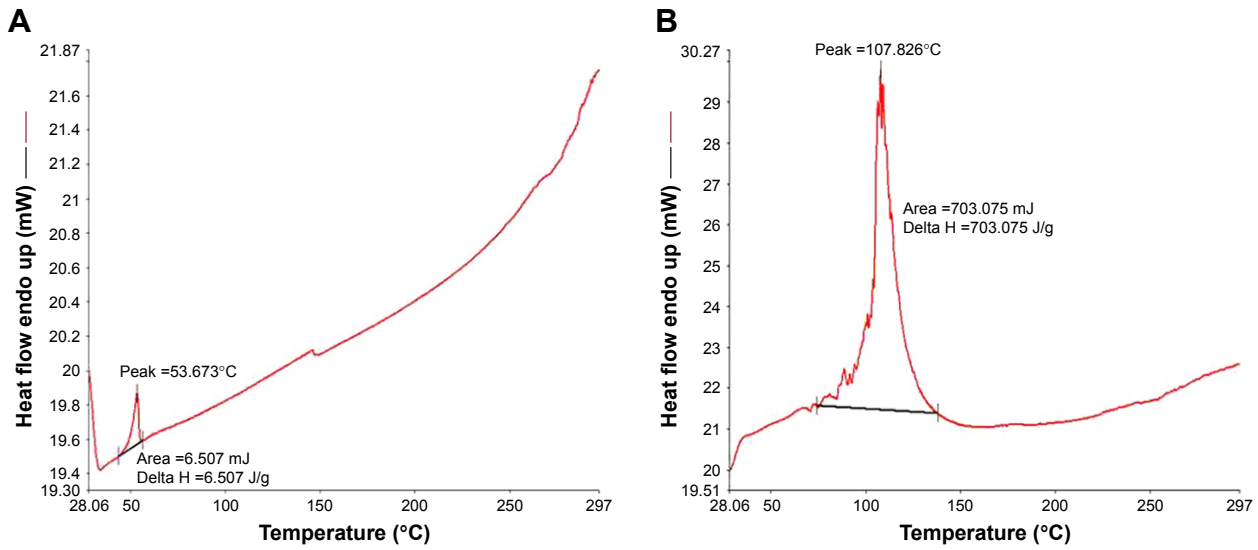

Figure S5 DSC thermograms of (**A**) NK and (**B**) optimized-formulation NKNPs.
Abbreviations: DSC, differential scanning calorimetry; NK, nattokinase; NKNPs, NK–poly(lactic-*co*-glycolic acid) nanoparticles.